JOURNAL OF APPLIED ELECTROCHEMISTRY **10** (1980) 203–211

Pressure effects on the performance and the e.m.f. of the Mg-AgCl seawater battery

M. HIROI

Chemical Laboratory, Kobe University of Mercantile Marine, Fukae-Minami, Higashinada, Kobe 658, Japan

Received 19 February 1979

The discharge curves of a magnesium–silver chloride seawater activated cell at different pressures were measured to examine the performance at great ocean depths. The e.m.f. measurements at increasing pressures were also carried out in order to understand the small differences in the discharge behaviour under different pressures and to get some information on the dissolution kinetics of magnesium in chloride solutions. The performance is shown at atmospheric pressure and at increased pressure and there is virtually no change in output power. It is found that Mg AZ61 is a better choice than Mg AZ31 at high pressures because of the nature of the sludge it forms. Partial molal volume changes for the magnesium oxidation reaction obtained with pure magnesium and its alloys (AZ31 and AZ61) in 0.5 M NaCl are presented and discussed.

1. Introduction

It is necessary for a seawater activated primary battery to function over a wide range of ocean environments; i.e., from 1.5% saline at 0° C to 3.6% saline at 30° C. In addition, the operation of the batteries at great ocean depths is becoming more important for such purposes as sophisticated electronic systems for military or scientific investigation, or life support systems for underwater habitats. There, however, seem to be few publications on the discharge characteristics at high pressures [1, 2]. The present study is intended to examine pressure effects on the discharge behaviour of Mg–AgCl cells. The following pressure effects have been considered; pressure effects on the e.m.f., the electrical conductivity of the electrolyte, and the solubility and gassing of hydrogen gas liberated from the chemical corrosion of the magnesium anode.

The results obtained from measurements of pressure coefficients of the e.m.f. serve as an experimental base for the interpretation of the electrochemical behaviour of magnesium [3, 4]. On the basis of $\overline{\Delta V}/n$ values for the magnesium oxidation reaction and the effect of chloride ion concentration on the corrosion potential and the corrosion rate, a mechanism involving the formation of magnesium monohydroxide (MgOH) as a reaction intermediate followed by the participation of chloride ions in the dissolution of magnesium is proposed.

2. Experimental

2.1. *Measurements of discharge curves*

Magnesium anodes, 10 mm × 15 mm, were made from Mg AZ31 (3% Al, 1% Zn) or Mg AZ61 (6% Al, 1% Zn) alloy plates (0.9 mm in thickness). Silver chloride cathodes were made from AgCl plates rolled to approximately 0.65 mm thickness. The surface was reduced by zinc powder prior to use. The size of the cathodes was the same as that of the magnesium anodes and the weight was about 0.47 g. Discharges were limited by the capacity of the silver chloride cathode.

Cells containing two anodes and one cathode were assembled with a 1 mm separation in a polyethylene cell; the vessels allowed the electrolyte of 3% sodium chloride to be separated from the oil which acted as a transmitter of pressure (cf. Fig. 1a).

Fig. 2 shows the pressure vessel used (cavity

0021–891X/80/020203–09$02.90/0

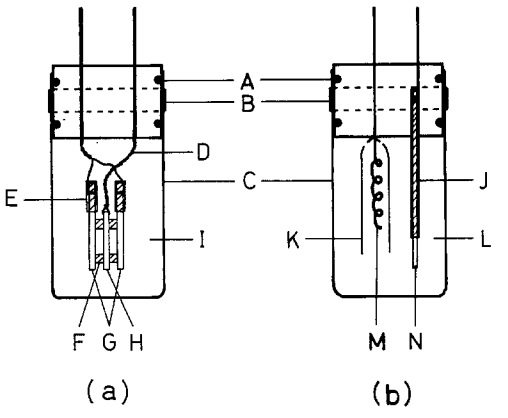

Fig. 1. Test cells. (a) cell for discharge tests, (b) cell for e.m.f. measurements. A, O-ring seal; B, fastening band; C, polyethylene cell vessel; D, silver lead; E, epoxy coating; F, 1mm separator; G, anode; H, cathode; I, 3% NaCl electrolyte; J, Teflon or epoxy coating; K, glass sleeve; L, 0.5 M NaCl electrolyte; M, Ag/AgCl electrode; N, anode.

dimensions 70 mm diameter by 50 mm). The lid of the vessel was equipped with two isolated electrical leads, a plug for a copper–constantan thermocouple and an air drain. Pressure was applied by a manual oil pump. The pressure was measured with a Bourdon gauge. The pressure chamber was set in an air bath maintained at $25 \pm 0.05^{\circ}$ C for all experiments and the temperature on the surface of cell vessel was monitored by the thermocouple.

Cells were discharged using constant current. Discharges were begun 4 h after pressure had been applied so that the temperature in the vessel had returned to ambient.

2.2. *Measurements of internal resistances*

The internal resistances during discharge were measured by a potential recovery method; namely, they were determined from the abrupt rise within 20 μs in cell voltage at the time when the discharge current was switched off. The change was recorded with a digital memory (Iwatsu, model DM305).

2.3. *E.m.f. measurements*

The cell used for e.m.f. measurements is shown in Fig. 1b. Runs were made using pure Mg(99.98%), Mg AZ31 and Mg AZ61 in 0.5 M NaCl solutions saturated with $Mg(OH)_2$. The solution was prepared by allowing a piece of Mg to corrode in the solution for a sufficient period of time to assure saturation. This electrolyte is buffered by the hydroxide equilibrium at a pH value near 10. Before each run the magnesium electrodes were immersed several times for about 10 s alternately in 7% HNO_3 and 1% HCl solutions and rinsed in a stream of distilled water and then dried.

Potentials were measured relative to a Ag/AgCl electrode. The electrodes were prepared by the method described by Hornibrook, Janz and Gordon [5]. Measurements of the e.m.f. were made by using a DVM (Hewlett Packard, model 34703A, 34750A) to 0.1 mV. After each change of pressure, 5–10 h were allowed for thermal and mechanical equilibrium to be re-established.

Considerable fluctuations in the e.m.f. (1–6 mV) were observed in some runs, especially in the case of cells with the Mg AZ61 anode. This

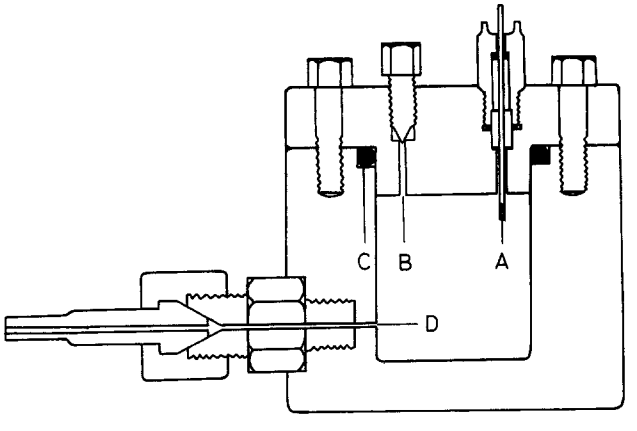

Fig. 2. Pressure vessel. A, electrical lead; B, air drain; C, O-ring seal; D, pressure inlet.

is considered to be caused by the gassing of hydrogen gas and peeling off of corrosion products.

The e.m.f. measurements were made 15 times at 30 s intervals and this set of measurements was repeated at least 5 times at 15 min intervals. Of the data recorded, the most frequently observed voltage was used as an e.m.f. at a given pressure. The fluctuations hindered the precise determination of the e.m.f. and the pressure coefficients, but the pressure effect could be seen qualitatively.

In order to check the method adopted and the instruments used, the e.m.f. of a cell

$$\text{Ag, AgCl}|0.5\text{ M NaCl}|\text{Hg}_2\text{Cl}_2\text{, Hg}$$

the reaction of which is well known and the volume change is precisely calculable, was measured. The average pressure coefficient of the three cells was 3.1 mV kbar^{-1}, corresponding to -3.0 cm^3 equivalent^{-1}, showing a good agreement with the calculated value of -2.7 cm^3 equiv^{-1}.

3. Results

Constant current discharge curves of Mg AZ31–AgCl and Mg AZ61–AgCl cells at 50 mA cm^{-2} (150 mA) at pressures ranging from atmospheric pressures to 980 bar (1000 kg cm^{-2}) are shown in Figs. 3 and 4, respectively. Values of the current efficiency of the AgCl cathode (i.e. % of AgCl consumed), instead of time, are plotted against the observed voltages in the figures. Discharges were also made at other currents (10, 20 and 100 mA cm^{-2}). The reason that only the discharges at 50 mA cm^{-2} are shown is that cells containing the Mg AZ31 anodes showed the most characteristic discharge behaviour at this drain rate.

In both cells the discharge voltages at high pressures are shown to be 20–30 mV higher than those at surface pressure and the electrical noise is shown to decrease at increasing pressure. The efficiency of the cathode used was generally 90% at this discharge rate. Cells using the Mg AZ61 anodes yielded discharge curves that were somewhat higher and flatter than cells containing the Mg AZ31 anodes. In the case of cells with the Mg AZ31 anodes, minima in the discharge curves were observed at a later stage of discharge. They were observed at a rate of 50 mA cm^{-2} and at pressures higher than 490 bar, but not at the other currents used.

Figs. 5 and 6 show the changes in the internal resistance during discharge at surface pressure and at 980 bar. The fluctuation of the internal resistance at the surface was violent, while at high applied pressures the internal resistance changed smoothly. In the case of cells with the Mg AZ31 anodes the resistance increased somewhat at a later stage of discharge. Obviously the fluctuation was caused by hydrogen gas bubbles formed on the Mg anodes.

Fig. 7 shows typical e.m.f.–pressure relationships. Volume changes for cells at pressures higher than 100 bar are shown in Table 1. The relation between the pressure coefficient of the e.m.f. $(\partial E/\partial p)$ and the volume change $(\overline{\Delta V})$ at constant temperature and constant chemical potential of all other species is given as

$$\overline{\Delta V}/n = -F(\partial E/\partial p)_{T,\mu} \qquad (1a)$$

or

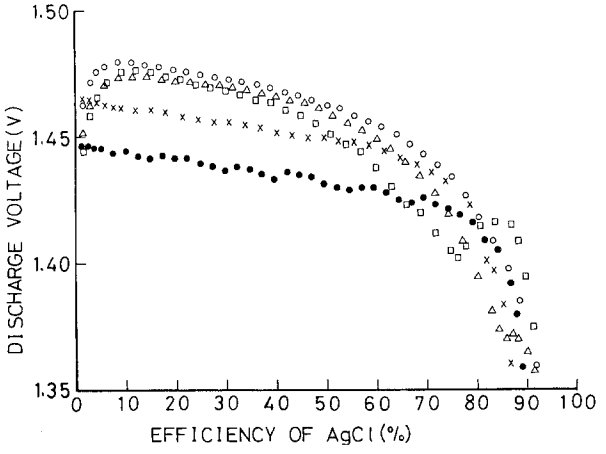

Fig. 3. Discharge curves of Mg AZ31–AgCl cells at different pressures. • atmospheric pressure, X 49, ○ 245, △ 490, □ 980 bar.

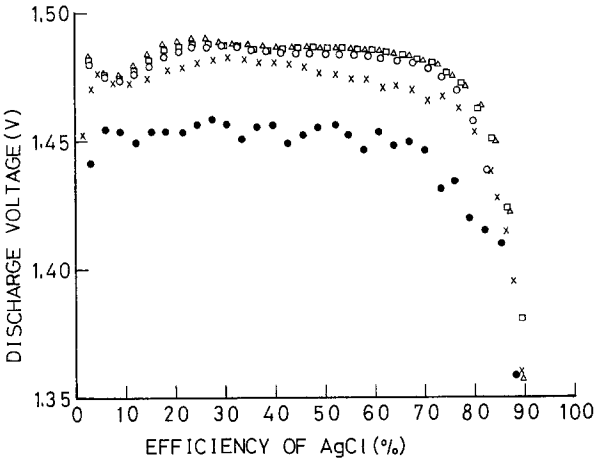

Fig. 4. Discharge curves of Mg AZ61–AgCl cells at different pressures. • atmospheric pressure, × 49, ○ 245, △ 490, □ 980 bar.

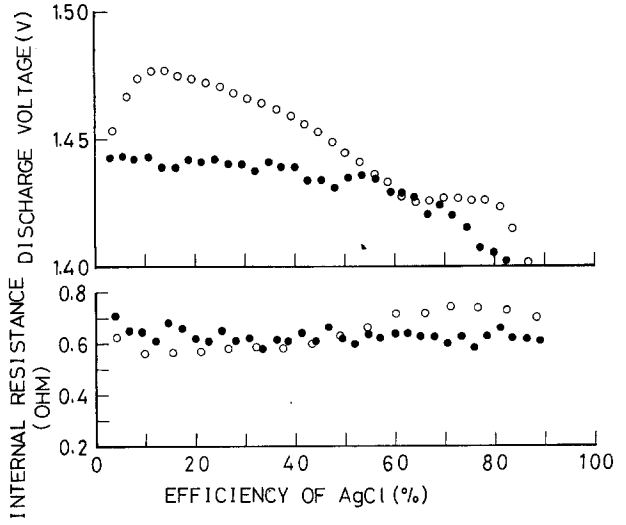

Fig. 5. Discharge curves and the changes in the internal resistance of Mg AZ31–AgCl cell. • atmospheric pressure, ○ 980 bar.

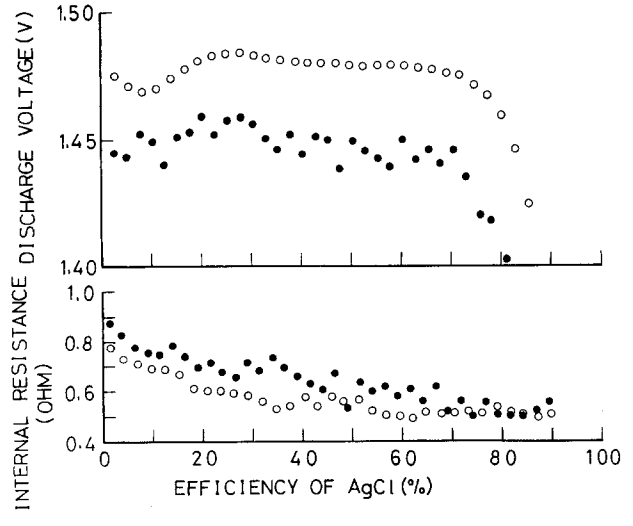

Fig. 6. Discharge curves and the changes in the internal resistance of Mg AZ61–AgCl cell. • atmospheric pressure, ○ 980 bar.

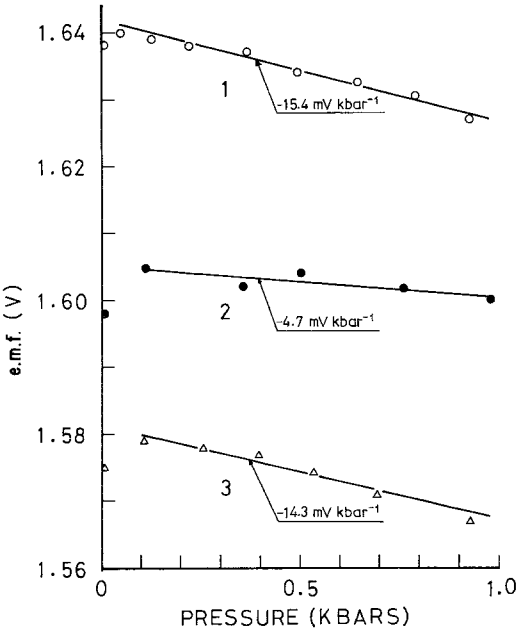

Fig. 7. Effect of pressure on the e.m.f. 1, pure Mg–AgCl/Ag; 2, Mg AZ61–AgCl/Ag; 3, Mg AZ31–AgCl/Ag.

$$\overline{\Delta V}/n \text{ (in cm}^3 \text{ mol}^{-1}) = -0.965(\partial E/\partial p) \quad \text{(in mV kbar}^{-1}) \qquad (1b)$$

where n is the number of electrons transferred and F is Faraday's constant. Thus $\overline{\Delta V}/n$ can be obtained from the slope of the e.m.f. versus pressure relationship. The slope was determined by the method of least squares.

The e.m.f. increased with increasing pressure up to about 100 bar and then decreased with pressure. The pressure coefficient of the e.m.f. should reflect changes of mechanism, but it seems unlikely that a change of mechanism occurs at such a low pressure. The cause of the changes of the pressure coefficient may be the hydrogen gas evolution.

Table 1. Experimental $\overline{\Delta V}/n$ values for Mg–AgCl, Ag cells with 0.5 M NaCl electrolyte saturated with $Mg(OH)_2$ (100–1000 bar)

Anode	$\overline{\Delta V}/n$ (cm³ equiv.⁻¹)	*Number of cells averaged*
Pure Mg	+ 14.3	4
Mg AZ31	+ 13.5	4
Mg AZ61	+ 4.4	3

Additional experiments on the corrosion potential (E_{corr}) and the corrosion current density (i_{corr}) for pure magnesium were also carried out to learn more about the mechanism of the dissolution process in Cl^- containing solutions since it was difficult to infer a reaction step controlling the rate or the electrode potential from values of $\overline{\Delta V}$ alone. The results in the solutions saturated with $Mg(OH)_2$ at atmospheric pressure are shown in Fig. 8, where values of the mean activity of NaCl ($a_{\pm NaCl}$), rather than concentration, are plotted against the observed potentials and the dissolution rates.

Cylindrical electrodes (2.0 cm in diameter and 1.5 cm in length) were made from a pure magnesium (99.98%) block and covered with a plastic coating, leaving 1.5 cm^2 of the surface exposed to the testing solution. A three-electrode cell (Hokutodenko, model HX-101) was used in this experiment. The auxiliary electrode (a platinum plate) compartment was separated from the test cell by a sintered glass disc. Potentials were measured against a saturated calomel electrode (SCE). The measurements were made in NaCl solutions saturated with $Mg(OH)_2$ in the concentration range 0.02–1 M. Before immersion of the test electrode, the test electrolyte was de-aerated for several hours with purified nitrogen.

The corrosion current density was determined by extrapolation of the cathodic Tafel line to the corrosion potential. The potential changed rapidly in the anodic direction in the initial 10 min and almost reached a steady state value in 30 min, consequently the potential after 30 min was used as the corrosion potential. More details of the experiment procedures can be found elsewhere [25].

Both the corrosion potential and the dissolution rate are a function of chloride ion concentration. This means that there is a need to consider the role that the chloride ion plays in magnesium corrosion. The experimental results shown in Fig. 8 can be summarized by the following expressions.

$$\left(\frac{\partial E_{corr}}{\partial \log a_{Cl^-}}\right)_{pH} = -81 \text{ mV decade}^{-1} \qquad (2)$$

$$\left(\frac{\partial \log i_{corr}}{\partial \log a_{Cl^-}}\right)_{pH} = 0.54 \qquad (3)$$

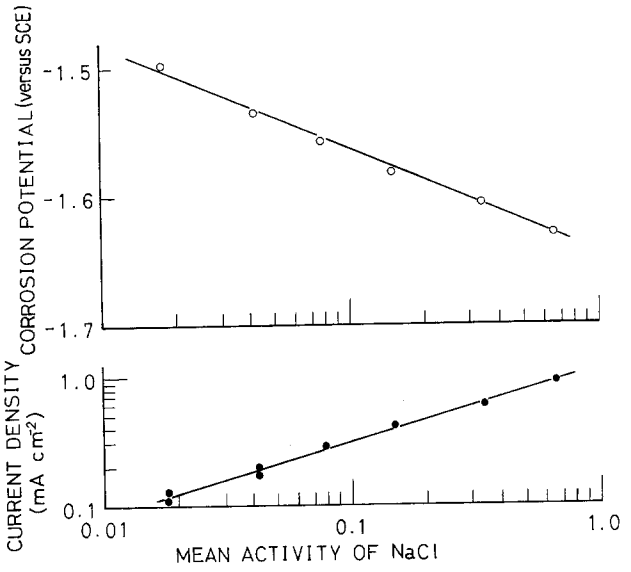

Fig. 8. Effect of Cl^- concentration on the corrosion potential and the corrosion current density of pure Mg at atmospheric pressure.

4. Discussion

4.1. *Pressure effects on the performance*

There may be many pressure effects on the discharge characteristics as mentioned earlier in this paper. One of the effects is that on the internal resistance caused by an increase of conductivity of the electrolyte. It is probably clear from the work of Körber that the electrical resistance of 0.5 M NaCl solution decreased with rising pressure up to about 2000 bar [4], but its contribution to the discharge voltage is not so large; it can be calculated to be about 5 mV.

The electrical noise is high at surface pressure, but it appears to decrease with increasing pressure. The noise is due to gas bubble formation. At high applied pressure large bubbles are not found since the hydrogen dissolves in solution. As approximately 23 cm^3 of the gas was evolved by 3 cm^2 of magnesium surface over a discharge period of 36 min and about 8 cm^3 of the electrolyte was used, hydrogen would be completely absorbed at pressures above 120 bar [6]. The Mg AZ61 anode liberated a little more hydrogen than the Mg AZ31 anode. This explains the higher fluctuation of the discharge voltages and the internal resistance of the cells with Mg AZ61 at surface pressure.

The absence of bubbles at high pressure seems to be most influential on the performance since the pressure effect on the e.m.f. is small and it seems that there are no significant effects of dissolved hydrogen on the discharge curves obtained.

The overall pressure effects on the discharges were small and, therefore, seawater activated batteries can be operated with virtually no change in discharge characteristics at great ocean depths.

There was a difference in discharge curves between cells with the Mg AZ31 anode and with the Mg AZ61 anode. This difference is a result of the nature of discharge products formed on the anode during discharge. The observations of the cells after discharge showed clogging between the plates in the case of Mg AZ31 anode. The sludge was rather dense and adhesive. A greyish-white product also formed on the Mg AZ61 anode, but it was a granular, rapidly settling sludge and not so adherent to the plate. The layer, therefore, remained thin on the Mg AZ61 anode even at high pressures. In the case of Mg AZ31 anode, the internal resistance increases at high applied pressures as the layer of the sludge grows. The layer reaches the opposite plate at a later stage of discharge. After that, the internal resistance remains constant or decreases somewhat on acount of the build-up of heat by the discharge current.

From these results, of the two magnesium anodes tested, Mg AZ61 is the better choice at high pressures as well as at surface pressure [7].

Table 2. Corrected experimental $\overline{\Delta V}/n$ values for the oxidation reaction of magnesium

Anode	$\overline{\Delta V}/n$ (cm³ equiv.⁻¹)	*Error*
Pure Mg	− 2	± 4
Mg AZ31	− 3	± 4
Mg AZ61	− 12	± 7

4.2. *Mechanism of magnesium dissolution*

In order to use the volume change to discuss reaction mechanisms, a value of $\overline{\Delta V}$ for the oxidation reaction of magnesium must be derived from the experimental values shown in Table I. $\overline{\Delta V}/n$ values for the silver–silver chloride reference electrode can be calculated to be + 7.7 cm³ equiv⁻¹. The change in the Ag/AgCl electrode potential caused by the change in activity coefficient due to the compressive effect must also be taken into account. It was calculated to be − 0.8 mV at 1000 bar, corresponding to a partial molal volume of + 0.77 cm³ for 0.5 M NaCl solution at 25° C [8]. In addition, the hydrogen evolution reaction

$$H^+ + e = \tfrac{1}{2}H_2(aq) \qquad (4)$$

proceeds simultaneously on the magnesium anode at equal rate to the corrosion process. $\overline{\Delta V}$ value for Reaction 4 is + 7.5 cm³ equiv.⁻¹ according to [1]. Table 2 gives the corrected values for the anodes studied. The value for Mg AZ61 obtained in this study is comparable to the value reported by Valeriote and Gallop [1]. Apparently alloy compositions affect the value of $\overline{\Delta V}/n$. The behaviour of Mg AZ61 in 0.5 M NaCl solution saturated with $Mg(OH)_2$ was different from that of pure Mg and Mg AZ31. Pure Mg and Mg AZ31 corroded more rapidly than Mg AZ61 which was subject to pitting and irregularities of attack.

Table 3

	Reaction	$\overline{\Delta V}/n$ (cm³ equiv.⁻¹)
	I	
(5)	$Mg \rightleftharpoons Mg^{2+} + 2e$	− 23.0
(6)	$Mg + 2H_2O \rightleftharpoons Mg(OH)_2 + 2H^+ + 2e$	− 18.2
(7)	$Mg + 2OH^- \rightleftharpoons Mg(OH)_2 + 2e$	+ 3.9
(8)	$Mg + H_2O \rightleftharpoons MgO + 2H^+ + 2e$	− 15.9
(9)	$Mg + 2OH^- \rightleftharpoons MgO + H_2O + 2e$	+ 6.2
(10)	$Mg + OH^- \rightleftharpoons MgO + H^+ + 2e$	− 4.9
(11)	$Mg + OH^- \rightleftharpoons MgOH^+ + 2e$	~ + 2
(12)	$Mg + H_2O \rightleftharpoons MgOH^+ + H^+ + 2e$	~ − 9
	II	
(13)	$Mg \rightleftharpoons Mg^+ + e$	~ − 20
(14)	$Mg^+ \rightleftharpoons Mg^{2+} + e$	~ − 26
(15)	$Mg^+ + 2H_2O \rightleftharpoons Mg(OH)_2 + 2H^+ + e$	~ − 16
(16)	$Mg^+ + 2OH^- \rightleftharpoons Mg(OH)_2 + e$	~ + 28
(17)	$Mg + OH^- \rightleftharpoons MgOH + e$	~ + 3
(18)	$Mg + H_2O \rightleftharpoons MgOH + H^+ + e$	~ − 19
(19)	$MgOH + OH^- \rightleftharpoons Mg(OH)_2 + e$	~ + 5
(20)	$MgOH \rightleftharpoons MgOH^+ + e$	~ + 1
	III	
(21)	$MgH_2 + 2OH^- \rightleftharpoons Mg(OH)_2 + H_2 + 2e$	+ 4.4
(22)	$MgH_2 + 2OH^- \rightleftharpoons Mg(OH)_2 + 2H^+ + 4e$	− 1.9
(23)	$MgH_2 \rightleftharpoons Mg^{2+} + 2H^+ + 4e$	− 15.3
(24)	$MgH_2 \rightleftharpoons Mg^{2+} + H_2 + 2e$	− 23.2
(25)	$MgH_2 \rightleftharpoons Mg^+ + 2H^+ + 3e$	~ − 12
(26)	$MgH_2 \rightleftharpoons Mg^+ + H_2 + e$	~ − 20
(27)	$MgH_2 + OH^- \rightleftharpoons MgOH + 2H^+ + 3e$	~ − 4
(28)	$MgH_2 + OH^- \rightleftharpoons MgOH + H_2 + e$	~ + 2
	IV	
(29)	$Mg + 2H_2O \rightleftharpoons MgO_2 + 4H^+ + 4e$	~ − 14
(30)	$Mg + 2OH^- \rightleftharpoons MgO_2 + 2H^+ + 4e$	~ − 2

These results suggest that different reactions take place and the state of the surface differs with each anode material. The results for pure Mg will be discussed here.

In order to interpret the results obtained, all of the electrochemical reactions controlling the electrode potential must be considered. The possible magnesium electrode reactions considered [9, 10] and their calculated values of $\overline{\Delta V}/n$ based on $\overline{V}^0_{H^+} = -5.4\,cm^3\ mol^{-1}$ at 25° C were as shown in Table 3.

The calculations were made from published values of partial molal volumes for the electrolyte [11–14] and density data [15–17]. Since partial molal volumes for $MgOH^+$ and Mg^+, and density data for MgOH and MgO_2 were unavailable, estimates of these values had to be made [12, 13]. Some reactions in which MgH is a reactant species were eliminated since MgH is a gas and it is not considered to be able to exist in aqueous solutions [9].

The experimental data for pure Mg and Mg AZ31 are consistent with $\overline{\Delta V}/n$ values for Reactions 10, 11, 17, 20, 22, 27, 28 and 30. These reactions should also be able to explain such properties of the magnesium electrode as the nobility of the observed potential in comparison with the standard potential, the delay phenomenon [18], the presence of finely divided particles of the metal in corrosion films [19, 20], the secondary hydrogen evolution and the reducing power of the anolyte [21], and the low anodic efficiencies [18, 21–24]. Moreover, those reactions do not predict the effect of halide ions in magnesium dissolution and hence additional reaction must be considered.

The following mechanism is proposed for magnesium dissolution in chloride media.

$$Mg + H_2O \rightleftharpoons MgOH_{ads} + H^+ + e \qquad (31)$$

$$MgOH_{ads} + 2Cl^- \rightarrow MgCl(OH)Cl^- + e \qquad (32)$$

(rate determining)

$$MgCl(OH)Cl^- + OH^- \rightarrow Mg(OH)_2 + 2Cl^- \qquad (33)$$

The intermediate, $MgOH_{ads}$, may react in other ways, such as in Reaction 20 similar to the Bockris mechanism for iron dissolution [30] and in the following reaction.

$$2MgOH \longrightarrow Mg(OH)_2 + Mg \qquad (34)$$

If the adsorbed intermediate, $MgOH_{ads}$, follows Temkin adsorption behaviour, the rate equation for the mechanism can be written as [31, 32]

$$i_a = k_a a^2_{Cl^-} a^{0.5}_{OH^-} \exp(FE/RT) \qquad (35)$$

and the rate expression for the hydrogen evolution reaction can be written as [33, 34]

$$i_c = k_c a_H + \exp -(2FE/5RT) \qquad (36)$$

based on the cathodic Tafel slope on pure Mg.

From Equations 35 and 36 the following expressions are obtained by setting $E = E_{corr}$ and $i_a = i_c = i_{corr}$.

$$\left(\frac{\partial E_{corr}}{\partial \log a_{Cl^-}}\right)_{pH} = -84\,mV\ decade^{-1} \qquad (37)$$

$$\left(\frac{\partial E_{corr}}{\partial pH}\right)_{Cl^-} = -63\,mV\ pH^{-1} \qquad (38)$$

$$\left(\frac{\partial \log i_{corr}}{\partial \log a_{Cl^-}}\right)_{pH} = 0.57 \qquad (39)$$

$$\left(\frac{\partial \log i_{corr}}{\partial pH}\right)_{Cl^-} = -0.57 \qquad (40)$$

These relationships agree reasonably well with the results obtained in this study (cf. Fig. 8) and the change in potential with pH reported by Perrault. Perrault [29] observed a −60 mV change in potential with each unit change in pH within the pH range of 7–12. However, Equation 35 has not yet been experimentally verified since the anodic Tafel slope for magnesium has not been determined precisely owing to the characteristics of the electrode [23, 25, 35], and it is not clear whether the corrosion rate is pH dependent in chloride media. According to the data obtained by Vermilyea and Kirk [36], the following relation could be derived within the pH range of 9–11 in $MgSO_4$ solutions.

$$\left(\frac{\partial \log i_{corr}}{\partial pH}\right) = -0.3 \qquad (41)$$

The value of $\overline{\Delta V}/n$ for Reaction 32 must explain the experimental values. The partial molal volume for $MgCl(OH)Cl^-$ was not known, so it had to be inferred from an estimated size. The value was taken to be approximately $+60\,cm^3$. The $\overline{\Delta V}/n$ value for Reaction 32 would be calculated to be $\sim -4\,cm^3$.

5. Summary

Seawater activated batteries with magnesium anodes are dependent on stirring induced by hydrogen evolution to remove the sludge from the battery and the gassing is dependent on pressure. At the pressure where gassing stops, the discharge behaviour begins to be affected by the nature of the sludge formed. The performance at great ocean depths can be expected to be similar to that at a temperature near 4° C, since pressure effects on the performance were found to be small. The rate expression for magnesium dissolution can be developed theoretically by a mechanism including the formation of magnesium monohydroxide followed by the participation of chloride ions in chloride media.

Acknowledgement

The author is indebted to the Yuasa Battery Co. Ltd for the magnesium alloys used in this study.

References

[1] E. M. L. Valeriote and L. D. Gallop, *J. Electrochem. Soc.* **121** (1974) 1245.
[2] F. P. Malaspina, *IECEC '75 Record* (1975) 817.
[3] G. J. Hills and P. J. Ovenden, in 'Advances in Electrochemistry and Electrochemical Engineering,' Vol. 4, (Edited by P. Delahay) Electrochemistry at High Pressures, Interscience, New York (1966).
[4] P. W. Bridgman, 'The Physics of High Pressure' Dover, New York (1970) pp. 372,360.
[5] W. J. Hornibrook, G. J. Janz and A. R. Gordon, *J. Amer. Chem. Soc.* **64** (1942) 513.
[6] 'Chemical Engineer's Handbook,' (Edited by R. H. Perry, C. H. Chilton and S. D. Kirkpatrick) 4th ed., 14-5, McGraw-Hill, New York (1963).
[7] W. N. Carson, W. H. Fischer and E. G. Siwek, *Electrochem. Tech.* **5** (1967) 423.
[8] S. Harned and B. B. Owen, 'The Physical Chemistry of Electrolytic Solutions,' 3rd edn., Reinhold Publishing Corp., New York (1958).
[9] G. G. Perrault, *J. Electroanal. Chem.* **27** (1970) 47.
[10] *Idem*, in 'Encyclopedia of Electrochemistry of the Element,' (Edited by A. J. Bard) VIII-4, Marcel Dekker, New York (1978).
[11] B. B. Owen and S. R. Brinkley, Jr., *Chem. Rev.* **29** (1941) 461.
[12] R. M. Noyes, *J. Amer. Chem. Soc.* **86** (1964) 971.
[13] F. J. Millero, in 'Water and Aqueous Solutions,' (Edited by R. A. Horne) Wiley–Interscience, New York (1972) ch. 13.
[14] J. V. Leyendekkers, 'Thermodynamics of Seawater,' Part 1, Marcel Dekker, New York (1976) ch. 4.
[15] 'Handbook of Chemistry and Physics,' 59th edn., Section B, CRC Press (1978–1979).
[16] D. A. Davenport, R. B. Fosterling and V. Srinivasan, *J. Chem. Ed.* **55** (1978) 93.
[17] B. Siegel and G. G. Libowitz, in 'Metal Hydrides,' (Edited by W. M. Mueller, J. P. Blackledge and G. G. Libowitz), Academic Press, New York (1968) ch. 12.
[18] J. L. Robinson and P. F. King, *J. Electrochem. Soc.* **108** (1961) 36.
[19] C. Brouchere, *J. Inst. Metals* **71** (1943) 131.
[20] M. E. Straumanis and B. K. Bhatia, *J. Electrochem. Soc.* **110** (1963) 353.
[21] R. L. Petty, A. W. Davidson and J. Kleinberg, *J. Amer. Chem. Soc.* **76** (1954) 363.
[22] W. J. James, M. E. Straumanis and J. W. Johnson, *Corrosion* **23** (1967) 15.
[23] J. W. Johnson, C. K. Chi and W. J. James, *ibid* **23** (1967) 204.
[24] P. F. King, *J. Electrochem. Soc.* **113** (1966) 536.
[25] M. Hiroi, *Denki Kaguka* (*J. Electrochem. Soc. Japan*) **41** (1973) 608.
[26] I. Iidaka, *Nippon Kaguka Zasshi* (*J. Chem. Soc. Japan*) **51** (1930) 301, 626.
[27] G. Wada, *ibid* **75** (1954) 170, 746.
[28] L. Whitby, *Trans. Faraday Soc.* **29** (1933) 415, 853, 1318.
[29] G. G. Perrault, *C. R. Acad. Sci.,Ser. C.* **280** (1975) 1069.
[30] J. O'M. Bockris, D. Drazic and A. R. Despic, *Electrochim. Acta* **4** (1961) 325.
[31] E. Gileadi and B. E. Conway, in 'Modern Aspects of Electrochemistry,' No. 3, (Edited by J. O'M. Bockris and B. E. Conway) Butterworths, London (1964) p. 381.
[32] R. J. Chin and K. Nobe, *J. Electrochem. Soc.* **119** (1972) 1457.
[33] E. J. Kelly, *ibid.* **112** (1965) 124.
[34] J. O'M. Bockris, in 'Modern Aspects of Electrochemistry,' No. 1, (Edited by J. O'M. Bockris) Plenum Press, New York (1968).
[35] H. A. Robinson, *Trans. Electrochem. Soc.* **90** (1946) 485.
[36] D. A. Vermilyea and C. F. Kirk, *J. Electrochem. Soc.* **116** (1969) 1487.